Journal of King Saud University – Science 35 (2023) 102843

HOSTED BY

Contents lists available at ScienceDirect

Journal of King Saud University – Science

journal homepage: www.sciencedirect.com

Original article

# A comparative cytological study of silver and molybdenum oxide nanostructures against breast cancer cells

Rizwan Wahab [a,*], Maqsood A. Siddiqui [a], Javed Ahmad [a], Quaiser Saquib [a], Abdulaziz A. Al-Khedhairy [a]

[a] Chair for DNA Research, Zoology Department, College of Science, King Saud University, Riyadh 11451, Saudi Arabia

ARTICLE INFO

*Article history:*
Received 12 May 2023
Revised 16 June 2023
Accepted 6 August 2023
Available online 11 August 2023

*Keywords:*
Molybdenum oxide NRs
Silver NPs
Cytotoxicity
MCF-7 cells
ROS
RT-PCR

ABSTRACT

Cancer is a denying disease, and among a number of cancers types, breast cancer is a recurrent in females, which affect word widely. For these reasons, the work presented here to show the comparative cytological responses of breast (MCF-7) cancer cells with silver and molybdenum oxide nanostructures. The nanostructures were produced via chemical process and characterized. The crystallinities, their size and phases were determined with X-ray diffraction pattern (XRD), while the structural details were scrutinized via scanning electron microscopy (SEM) and transmission electron microscopy (TEM) correspondingly. The nanorods (NRs) and nanoparticles (NPs) were exhibit and confirmed individual diameter of ~50–60 nm and ~15 nm separately. A cytotoxicity's studies of MCF-7 cells were sway and reliant to their doses (1 to 100 μL/mL) with α-$MoO_3$NRs and AgNPs established via 3-[4,5-dimethylthiazol-2-yl]-2,5 diphenyl tetrazolium bromide (MTT) and Neutral Red Uptake (NRU) assays. The reactive oxygen species (ROS) were also upsurges slowly from 105, 124, 132, 148 and 108, 130,135, 165 with dissimilar concentrations of α-$MoO_3$NRs and AgNPs (25, 50 and 100 μL/mL) with control reciprocally. Also gene expression (mRNA extraction) study with apoptotic markers in presence of α-$MoO_3$NRs and AgNPs were up-regulated and shows apoptosis in cells. The study provides a possible comparative results related to the cytotoxicity's in breast (MCF-7) cancer cell with AgNPs are high as compared to α-$MoO_3$NRs also authenticated via gene expression study.



## 1. Introduction

Among a number of cancers types, the breast cancer is very common to the whole world and affected especially in female candidate (Nardin et al., 2020). As it's known that cancer is a denying disease affect not only the particular organ but also affect the whole body system (Wahab et al., 2013). An estimated value of the breast cancer, grasp a more than one million women's world wide. A detailed statistical data reveals that cancer increase very widely for instance in 2008, ~421,000 cases were diagnosed for cancers, ~49,500 cases were found in 2009–2010 only in Europe. The breast cancer cases is increases day by day and a new cases (~268,600) were identified in women, also detected in men (~2,670) in 2019 (Nardin et al., 2020). From this divesting disease an average 42,170 women in U.S. to die in 2020 (Breast Cancer Facts & Figures 2019-2020). A number of techniques have been used to control the disease such as chemotherapy, radiotherapy, proton beam therapy, hormone therapy, targeted drug therapy, immunotherapy etc, that causes so much suffering (Chen et al., 2020, Cammarata et al., 2020, (Boing et al., 2020), Li et al., 2020). With various therapies, the surgery is also an option to remove the cancer cells from the particular organ of the body (He et al., 2020, Wahab et al., 2014).

Although numerous options are available to cure from cancer disease but the cost of the therapies or surgery is very high for the low income families. Recently, the material science and especially the nanotechnology, which is an interdisciplinary area of research and it's a best alternative for to diminish the cancer cells at a very low cost, much effective opposed to cancer cells and not to harm the body system. Towards to this direction a number of cytological studies were conducted with using nano and

* Corresponding author at: College of Science, Zoology Department, P.O. Box 2455, King Saud University, Riyadh 11451, Saudi Arabia.
*E-mail address:* rwahab@ksu.edu.sa (R. Wahab).

Peer review under responsibility of King Saud University.

Production and hosting by Elsevier

https://doi.org/10.1016/j.jksus.2023.102843
1018-3647/

microstructures with different oxides and metal NPs for to retard the proliferation of cells such as cobalt oxide NPs were employed for PDTs and cytotoxic effects of materials against HepG2 cells (Iqbal et al., 2020). In other report, Bozinovic et al. describes the effect of $MoO_3$NPs on human keratinocytes, with HaCaT cells via cytotoxicity, apoptosis in cells, DNA damage, ROS, and cell-survival and inflammatory signaling pathways (Božinović et al., 2020). The antimicrobial studies were also conducted against *S.aureus*; *E.coli*, and *P.aeruginosa* by activating membrane stress in pathogens with using molybdenum trioxide. The molybdenum trioxide ($\alpha$-$MoO_3$) NPs were also used to study the selective cytotoxicity towards cancer cells via mitochondrial-mediated apoptotic pathway (Indrakumar and Korrapati, 2020). Including NPs, degradable nanosheets of $MoO_3$ structures were also utilized for the invasive cancer treatment (Qiu et al., 2021). Along with metal oxides, a number of prominent studies were conducted with metal based nanoparticles against cancer cells such as silver NPs were used to check the in cytological change against human liver (HepG2) and breast (MCF-7) cancer cells with MTT, NRU assay and changes in apoptotic genes were measured by qPCR study (Al-Khedhairy and Wahab, 2022).

A number of utilities of nanostructures were applied for innumerable objectives whereas a very limited studies are available to show the comparison of oxide and metal based nanostructures for cellular cytotoxicity studies with control and gene expressions. To keep this view, the aim of this work is to expound the role of oxide ($\alpha$-$MoO_3$NRs) and metal (AgNPs) based nanostructures against breast cancer cells. The structures were synthesized via solution method and characterized. The cytotoxicity's studies were showed against breast cancer cells (MCF-7) with using oxide and metal nanostructures. Here, the breast cancer cell lines (MCF-7 cells) were selected because this cancer has a major health problem worldwide. MTT and NRU assays were selected to check the viabilities of cancer cells (MCF-7) whereas apoptosis in cells caused with $\alpha$-$MoO_3$NRs and AgNPs were investigated with the available RT-PCR study. Here, we have also explained why the NPs are much useful to reduce the growth rate of cancer cells.

## 2. Experimental

### 2.1. Material and methods

#### 2.1.1. Synthesis of molybdenum oxide nanorods ($\alpha$-$MoO_3$NRs)

The molybdenum oxide ($\alpha$-$MoO_3$) nanorods were conducted with the use of ammonium heptamolybdate tetrahydrate $(NH_4)_6Mo_7O_{24}{\cdot}4H_2O$) and sodium hydroxide (NaOH) via solution process as per previously published literature with minor modification (Wahab et al., 2020). In a typical experiment $(NH_4)_6Mo_7O_{24}{\cdot}4H_2O$ (4 mM, ~0.494 g) and NaOH (0.15 M, ~0.6 g) were dissolved in 100 ml double deionized distilled water saprately. The pH of the solution was measured and it touches to 12.4, thereafter, the solution was refluxed in 250 ml capacity refluxing pot for 70°C for 60 min. Once the reaction was accomplished, the precipitate was kept for cooling at 25°C for ~24 h. The aqueous solution with precipiated product was transferred in a centrifuge tubes (~50 mL) and centrifuge at 3000 rpm for 3 min (Eppendorf, 5430R, Centrifuge, Germany) to remove the chemical impurities. Dried at room temperature in a glass petri dishes and to keep for the analysis.

#### 2.1.2. Synthesis of silver nanoparticle (AgNPs)

The AgNPs were prepared with the use of silver nitrate $AgNO_3$ (~0.01 M) and trisodium citrate (~3 mM) in 50 mL capacity beaker as described previously with minor modification (Al-Khedhairy and Wahab, 2022). The reaction mixture was transferred to the black chamber, where no light enters. Keep the solution till the color changes initially brownish and then black, this change indicates the formation of AgNPs in the solution. The AgNPs was characterized well in terms of their physical and chemical characteristics.

#### 2.1.3. Characterizations

The XRD (PAN analytical XPert Pro, U.S.A.) was used to identify the crystal phases, size and crystallinity of the material with $Cu_{K\alpha}$ source ($\lambda$ = 1.54178 Å) from 30 to 90° with 40 kV/40 mA and 6°/min angle rotation. The structured of the synthesized materials were analyzed via SEM (JSM-6380 LA, Japan) TEM (JEOL JEM JSM 2010, Japan) as described hitherto (Wahab et al., 2014, 2020).

### 2.2. Cell culture

The cell culture was conducted with using breast cancer cells (MCF-7) grown in a medium (DM EM/MEM) including 12 % fetal bovine serum (FBS), 0.2% sodium bicarbonate, and antibiotic–antimycotic solution (100 X, 1 mL/100 mL) with humid environment (5% $CO_2$ & 95% $O_2$) at 37 °C. As per the previously reported work

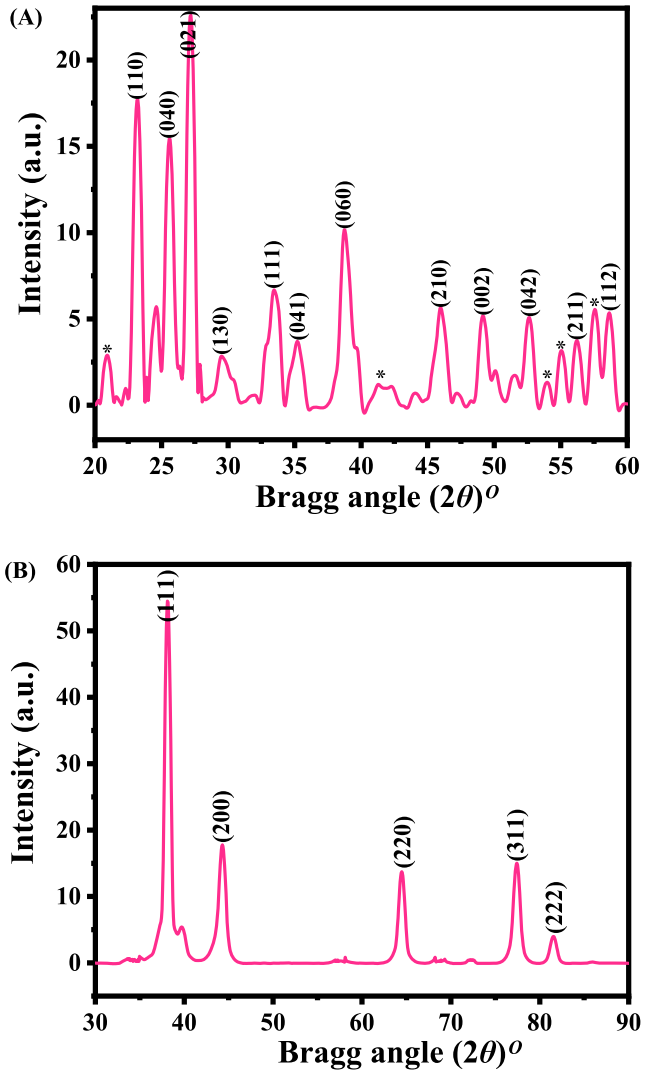


**Fig. 1.** Shows the XRD pattern of $\alpha$-$MoO_3$ (A) and AgNPs (B) respectively. Whereas*shows the unidentified peaks in the spectrum.

(Siddiqui et al., 2008), the viability of cells were evaluated by trypan blue dye and it express that more than 95% achieved viability of the cells were used in this study. Here, the cells were used between 10 and 12 passages and to treat the cells with α-$MoO_3$NRs and AgNPs, used at high concentration and diluted further at desired concentrations for the exposure of cells. The cells were plated in 6-well or 96-well plates as per the experimental requirement.

### 2.3. Reagents and consumables

The 3-(4, 5-dimethylthiazol-2-yl)-2, 5 diphenyltetrazolium bromide which is known as MTT assay, procured from Sigma Chem.Co. USA and recycled without any alternation except dilution. Culture medium such as Dulbecco's Modified Eagle Medium (DMEM) and MEM, antibiotics-antimycotic and FBS were bought from Invitrogen, USA. The plastic wares and other consumables products for cells culture were used from Nunc, Denmark.

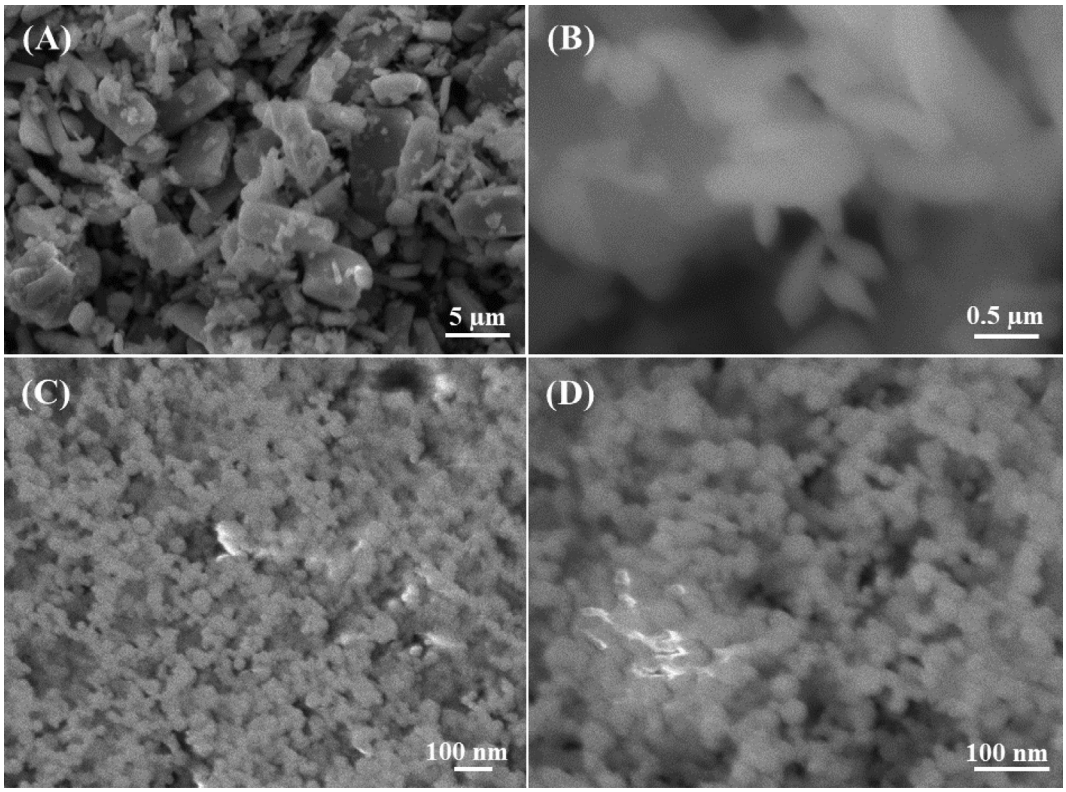


**Fig. 2.** SEM images of α-$MoO_3$: (A captured at 3000x and B at 27,000x) magnification whereas (C captured at 30000x and D at 60,000x) shows the AgNPs size. The estimated size of an individual NR diameter is ~50 nm and length is ~1–2 µm whereas individual NP size is ~15 nm respectively.

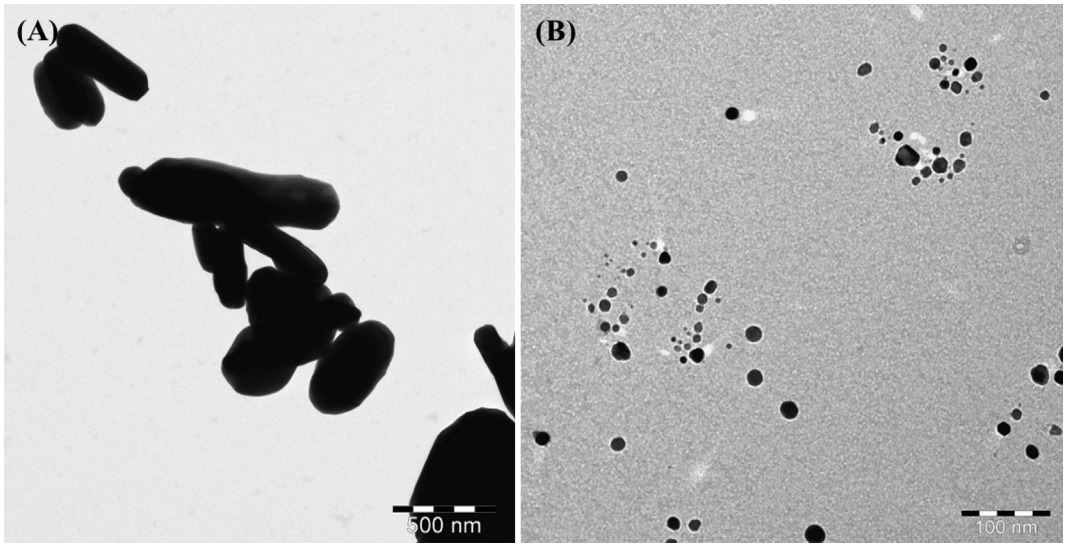


**Fig. 3.** TEM displayed the images of α-$MoO_3$NRs (A captured at1000x) and AgNPs (B captured at 50000x) respectively.

### 2.4. Cytotoxicity assessment by MTT assay

The breast cancer cells viabilities (MTT assays) with and without use of nanostructures (α-$MoO_3$NRs and AgNPs) were measured as earlier protocol (Siddiqui et al., 2008, Mosmann, 1983). For this, at initial the cells were sowed in 96 well plates (rate of $1 \times 10^4$/ well) with permissible to follow for 24 h at 37 °C with moist environment. Here, the cells were completely exposed with nanostructures (α-$MoO_3$NRs and AgNPs) 1–100 μg/mL for 24 h. Once the cells were inter mixed completely exposed in well plates, stock solution of MTT (5 mg/mL in PBS) was incorporated with rate of 10 μL/well in 100 μL of cell suspension and these cells were further incubated for 4 h. As the incubation was reached to their completion, the well plate's solution was with draw from the pipette and in these wells ~200 μL of dimethyl sulfoxide (DMSO) was mixed for to aspirate the formazan product and mixed gently. Solutions optical characteristic was measured at 550 nm with micro-plate reader (Multiskan Ex, Thermo Scientific, Finland). With treated samples, the control cells were also measured as a reference and to run with same parameters. The maximum absorbance depends upon used solvent in sample solution and the level of viability of cells % was calculated as per the equations mentioned below:

$$\% \text{ viability} = [(\text{total cells} - \text{viable cells})/\text{total cells}] \times 100$$

### 2.5. NRU assay

Including the MTT assay, the treated (α-$MoO_3$NRs and AgNPs) and untreated cells (only MCF-7 cells) cytotoxic optical characteristic were also confirmed via neutral red uptake (NRU) assay as described previously (Borenfreund and Puerner, 1985; Siddiqui et al., 2010). The MCF-7 cells ($1 \times 10^4$/ well) were sowed in a specified 96 well plates. When the cells were completely grown (after 24 h), these cells were exposed with both samples at desired conc (1–50 μg/mL) and to kept for 24 h in an incubator. After the exposure was finished, the cells were again incubated in NR medium (50 μg/mL) for 3 h. Then the cells were completely washed and dye were removed from both samples in 1% acetic acid and 50% ethanol solution. The optical intensity of the develop color was analyzed at 540 nm.

### 2.6. Reactive oxygen species (ROS)

The ROS generation were measured with using 2, 7-dichloro dihydrofluoresce in diacetate (DCF H-DA; procured from Sigma Aldrich, USA) dye as a fluorescence agent as described method previously (Zhao and Riediker, 2014). The cells were exposed with both nanostructures for 24 h and thereafter, cells were rinsed well with PBS and further nurtured for 30 min in DCFH-DA (20 μM) in dark place at 37 °C. The reaction of DCFH-DA dye with cells as control and treated cells were completed, and examined with using fluorescence microscope.

### 2.7. Gene expression study

The extraction of RNA was performed with cultured cells of MCF-7 cells in a 6-well plates control and treated samples at concentration of 50 μg/mL for 24 h. For this process, the RNeasy mini Kit (Qiagen) was used to mine the RNA as per protocol instructed from manufacturer's. The cDNA was synthesized from treated and untreated cells taking 1 μg of RNA by Reverse Transcriptase kit using MLV reverse transcriptase (GE Health Care, UK) as described protocol. The RT-PCR was completed on Roche® Light Cycler®480 (96-well block) (USA) followed with cycling program recommended. 2 μL (40 ng) of cDNA template included the 20 μL volume to this reaction mixture (Ahmad et al., 2022).

## 3. Result and discussion

### 3.1. X-ray diffraction pattern (XRD)

Fig. 1(A and B) shows the XRD of molybdenum oxide (α-$MoO_3$) and silver nanoparticles (AgNPs) correspondingly. From the XRD (Fig. 1A), well assigned peaks were identified in XRD, which are related to orthorhombic structures and analogous with the JCPDS data card no. 05-0508 and crystal lattice constants are $a$ = 3.962 Å, $b$ = 13.858 Å and $c$ = 3.697 Å respectively. The spectrum shows a peaks identified at defined places such as 23.21°⟨110⟩, 25.57° ⟨040⟩, 27.14° ⟨021⟩, 29.56°⟨130⟩, 33.44° ⟨111⟩, 35.29° ⟨041⟩, 38.78°⟨060⟩, 45.99°⟨210⟩, 49.08°⟨002⟩, 52.59°⟨042⟩, 54.95°⟨211⟩ and 58.59°⟨112⟩ respectively. The observed peaks are very similar to the crystalline α-$MoO_3$, except any other impurities (Wahab et al.,

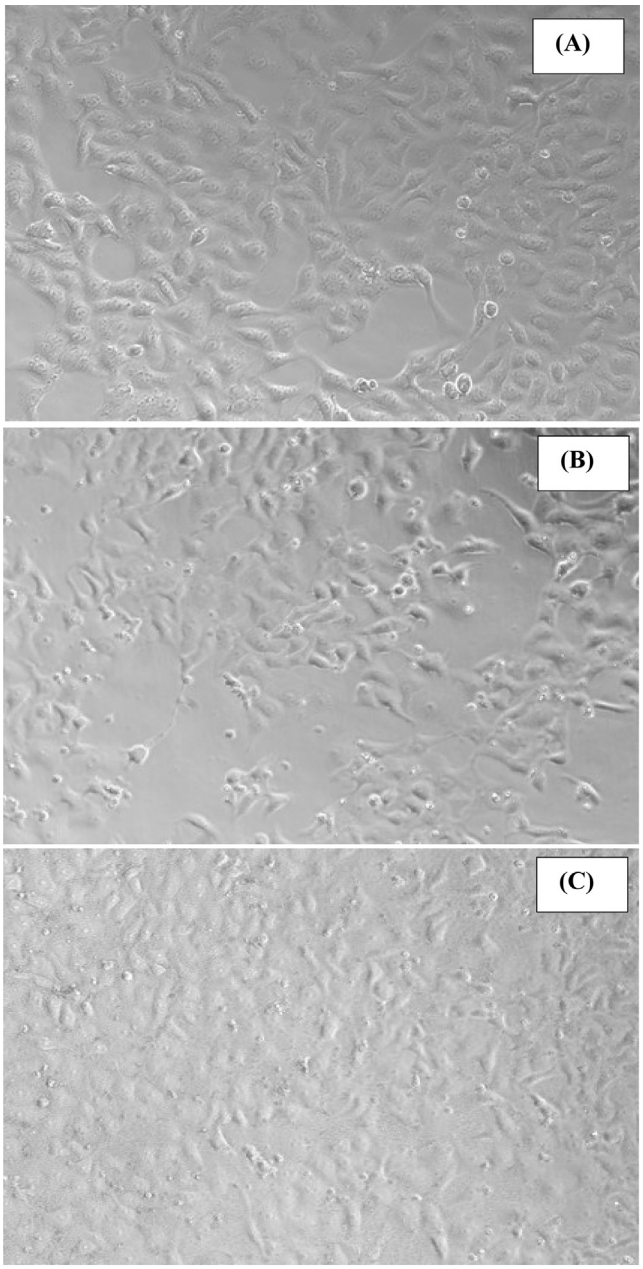


**Fig. 4.** The morphology of the MCF-7 (control A) and their structural change exposed with α-$MoO_3$NRs (B) and AgNPs (C) for 24 h. Images were captured under the phase contrast inverted microscope.

2020). The estimated size of the each crystallite is ~50 nm, calculated with using sherrer formula. Fig. 1(B) shows the XRD pattern of AgNPs are alike to the face centered cubic (FCC) structure with metallic silver and similar to the JCPDS card no. 04–0783 with crystal lattice constant is $a$ = 0.4086 nm correspondingly. The spectrum illustrates the indexed and assign peaks with their related positions such as 38.17° ⟨111⟩, 44.29°⟨200⟩, 64.40°⟨220⟩, 77.37°⟨311⟩ and 81.49°⟨222⟩ espectively, with an individual crystallite size was ~15 nm (Al-Khedhairy and Wahab, 2022).

### 3.2. Morphological studies of α-$MoO_3$NRs and AgNPs

#### 3.2.1. SEM results

The structural detail of the products were examination with SEM images captured at low and high magnification scale and presented as Fig. 2. At low magnified scale image (Fig. 2A) of α-$MoO_3$NRs shows the formation of several rod shaped structures that are arranged in manner as composed to form circular spheres shaped structure. The image was further identified at high scale which show the individual structure (Fig. 2B). It observed from the images that the average diameter of an individual NRs is in range of ~50–60 nm, whereas length exceeds to 1–2 μm (Fig. 2B). In other images captured at low (Fig. 2C) and high (Fig. 2D) scale magnification shows several AgNPs are arranged on the whole surfaces. The average size of each NP is ~15 nm, which smooth surface morphology.

#### 3.2.2. TEM results

Further for more clarification, the samples were also analyzed with TEM and represent as Fig. 3A. A number of several rods shaped structure of α-$MoO_3$ are appeared on surfaces with an average diameter is ~50–60 nm and 1–2 μm length respectively. In other image shows a number of small particles with nanometer scale is seen with an individual size is ~15 nm (Fig. 3B). The obtained images authenticated that the NPs surfaces are smooth, clear and are fully consistent with SEM analysis (Fig. 2).

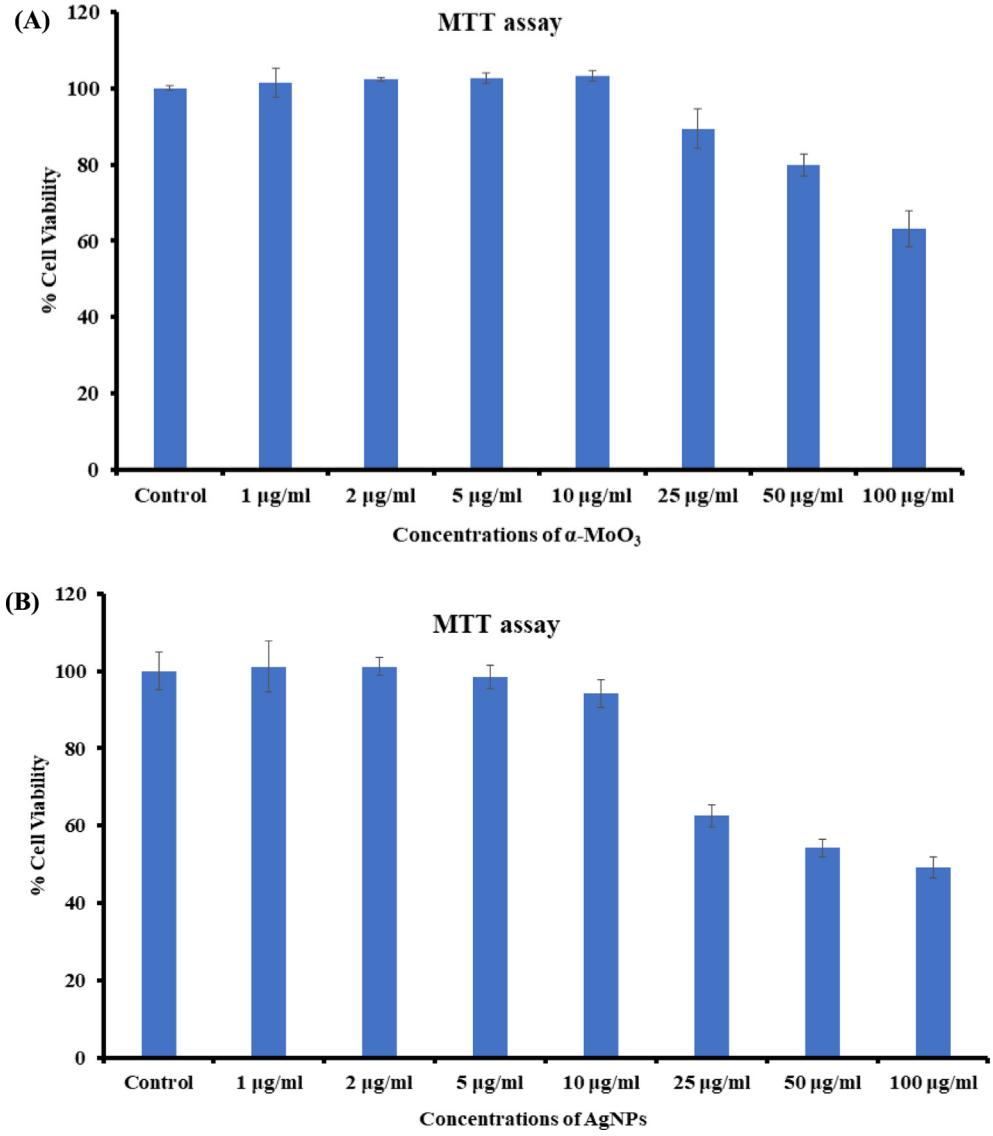


**Fig. 5.** Cytotoxicity study via MTT assay in MCF-7 cells succeeding the exposure of α-$MoO_3$NRs (A) and AgNPs (B) for 24 h. The experiments were conducted in triplicate manner (Mean ± SD triplicate).

### 3.3. General morphology of cancer cells (MCF-7) and their change with used nanostructures

The cells were cultured as described above protocol and the morphological study was observed via microscopy at 24 h incubation periods at 100 μg/mL of nanostructures (Fig. 4). The captured image of MCF-7 cancer cells (Fig. 4A-Control) whereas others images were captured with treated samples at 100 μg/mL concentration of α-$MoO_3$ (Fig. 4B) and AgNPs (Fig. 4C) respectively. From the observed images, it represents that the cells were nucleated and once their confluences reached to their enhanced confluence (∼70–80 %,) treated with nanostructures (α-$MoO_3$NRs and AgNPs) and analyzed. The observation reveals that there is no noteworthy change was noticed at an initial range of concentration of the nanostructures (1, 2, 5, 10 and 25 μg/mL data not shown), but once the concentration of α-$MoO_3$ and AgNPs upsurges to 50 to 100 μg/mL, the growth of the cells were much affected. The microscopic images authenticated that the cells were damaged with the incorporation of α-$MoO_3$NRs and AgNPs.

### 3.4. The induced cytotoxicity (MTT assay) with processed α-$MoO_3$NRs and AgNPs

As described in the material and method section that the untreated (control) breast cancer cells (MCF-7) and treated cells (MCF-7 cells with nanostructures) samples were exposed in a range of different concentrations from 1 to 100 μg/mL for 24 h incubation. The cytotoxicity's were examined through MTT assay. The obtained optical densities data shows viability of cancer cells were diminished with the incorporation of α-$MoO_3$NRs and AgNPs and these data's were concentration/dose-dependent. In case of α-$MoO_3$NRs, the MCF-7 cells viability, MTT assay was decreases at 24 h 101%, 102%, 102%, 103%, 89%, 79% and 63% (Fig. 5A) for the conc of 1, 2, 5, 10, 25, 50 and 100 μg/mL correspondingly

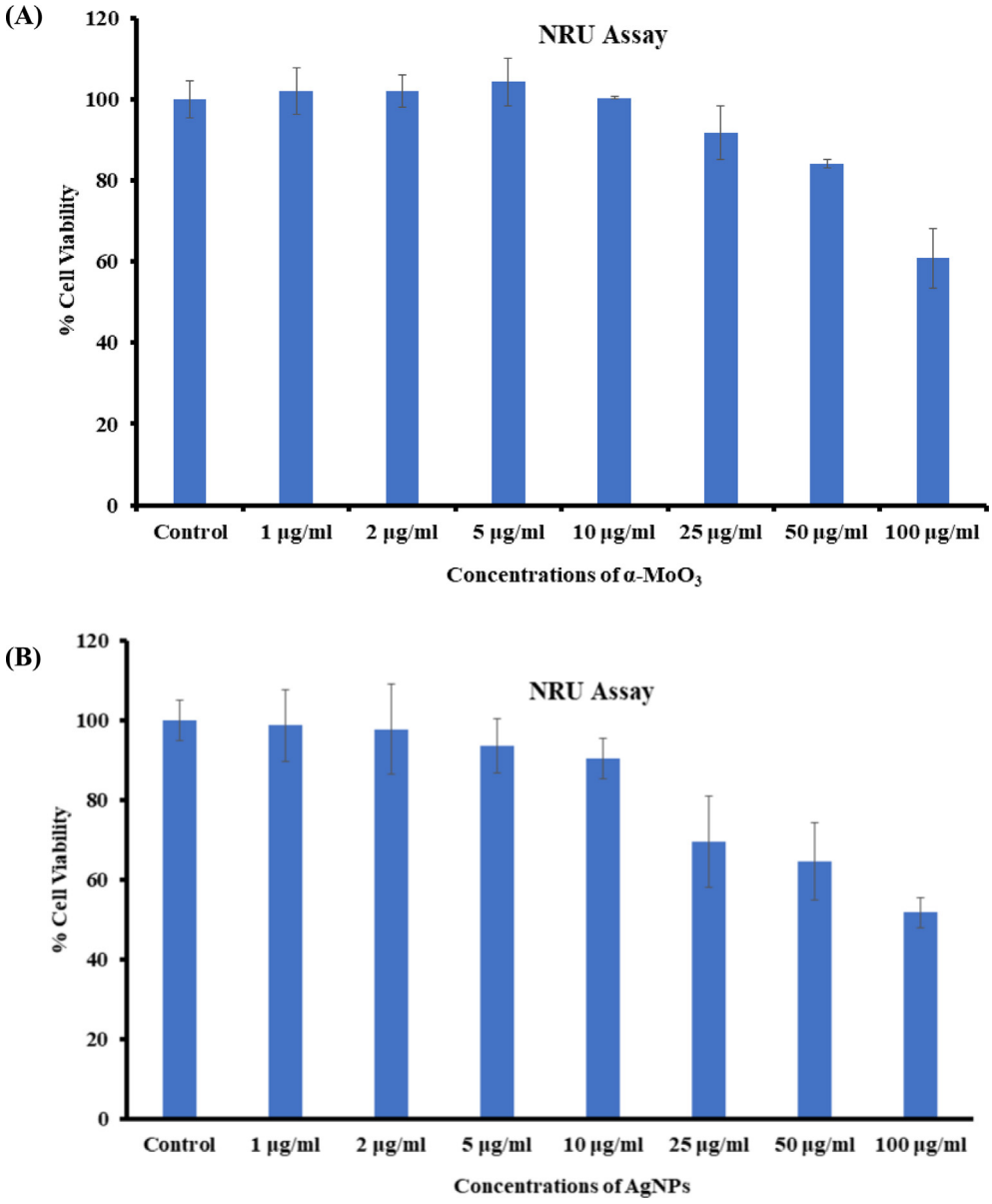


**Fig. 6.** Cytotoxicity study via NRU assay in MCF-7 cells succeeding the exposure of α-$MoO_3$NRs (A) and AgNPs (B) for 24 h. The experiments were conducted in triplicate manner (Mean ± SD triplicate).

($p < 0.05$ for each). In case of AgNPs, the MCF-7 cells viability, MTT assay was decreases at 24 h 101%, 101%, 98%, 94%, 62%, 54% and 49% (Fig. 5B) for the conc of 1, 2, 5, 10, 25, 50 and 100 μg/mL correspondingly ($p < 0.05$ for each). The recovered data's shows that cells viabilities were not much affected at initial concentration, whereas when the conc/doses of α-$MoO_3$NRs and AgNPs were exceeded to their optimum level, the cytotoxicity's were much influenced (Siddiqui et al., 2008).

### 3.5. Cytotoxicity study via NRU assay in MCF-7 cells with rods and nanoparticles shaped nanostructures

Apart from the MTT assay, the cytotoxic measurements were also verified non-treated and treated nanostructures via NRU assays as detailed in the materials and method. A similar observation were also found in NRU assays. As described in the MTT section, the NRU data also in consistent and shows that that the viabilities of cancer cells at initial conc of nanostructures (α-$MoO_3$NRs and AgNPs) were not much influenced, whereas once the conc increases, the growth of cancer cells were reduced. In case of α-$MoO_3$NRs, for the MCF-7 cells, NRU assay was decreases at 24 h 102%, 101%, 104%, 100%, 91%, 84% and 60% (Fig. 6A) for the conc of 1, 2, 5, 10, 25, 50 and 100 μg/mL correspondingly ($p < 0.05$ for each). In case of AgNPs, for MCF-7 cells, NRU assay was decreases at 24 h 98%, 97%, 93%, 90%, 69%, 64% and 51% (Fig. 6B) for the conc of 1, 2, 5, 10, 25, 50 and 100 μg/mL correspondingly ($p < 0.05$ for each) (Siddiqui et al., 2010).

### 3.6. Induced ROS generation in MCF-7 with nanorods and nanoparticles

A similar and sequential trends were also observed in ROS generations detected in MCF-7 cells after the exposure of α-$MoO_3$ and AgNPs at 25 to 100 μg/mL concentrations for 24 h (Fig. 7). The ROS is increases with AgNPs and it's evident from the image (Fig. 7A) as compared to control cells. An increase of 108%, 125% and 160% of ROS generation were observed with the interaction of α-$MoO_3$ in MCF-7 Cells at 25, 50 and 100 μg/mL, as compared to control (Fig. 7B). The ROS formed more 118%, 135% and 177% with the interaction of AgNPs at 25, 50 and 100 μg/mL conc. in MCF-7 cells as compared to control in 24 h (Fig. 7B) (Zhao and Riediker, 2014).

### 3.7. Gene expressions study with apoptotic and anti-apoptotic markers

The real time PCR was utilized for to understand the mRNA levels of apoptotic and anti-apoptotic marker genes (e.g. p53, Bax, caspase-3, caspase-3 and Bcl-2) in MCF-7 cells interacted with both α-$MoO_3$NRs and AgNPs at 50 μg/mL for 24 h. A noteworthy changes were observed in mRNA levels in apoptotic markers (p53, Bax, casp-3, casp-9 and Bcl-2) genes in MCF-7 cells, once exposed with α-$MoO_3$NRs and AgNPs (Fig. 8). The mRNA tumor suppression gene supports the apoptosis induction by α-$MoO_3$NRs and observed the enzymatic activities of caspase-3 at the conc of 50 μg/mL. The obtained results of mRNA gene expression with all chosen gene were in down-regulation and the fold changes for the p53 (2.7), Bax (3.3), Casp-3 (2.3), Casp-9 (2.6) and Bcl-2(0.71) in α-$MoO_3$NRs whereas in case of AgNPs the gene

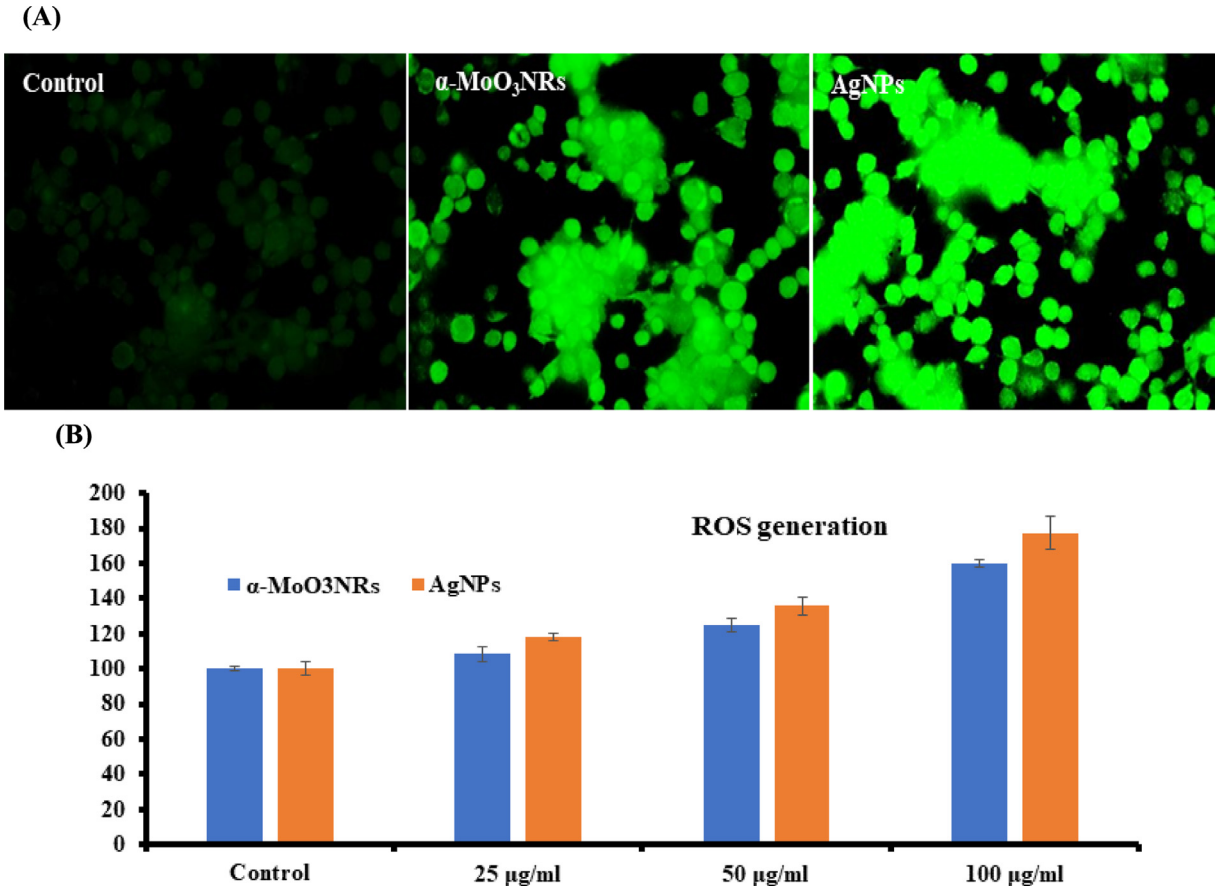


**Fig. 7.** (A) Representative images of α-$MoO_3$NRs and AgNPs induced ROS in MCF-7 cells exposed for 24 h. (B) Percent change in ROS with MCF-7 at varied conc of α-$MoO_3$NRs and AgNPs respectively.

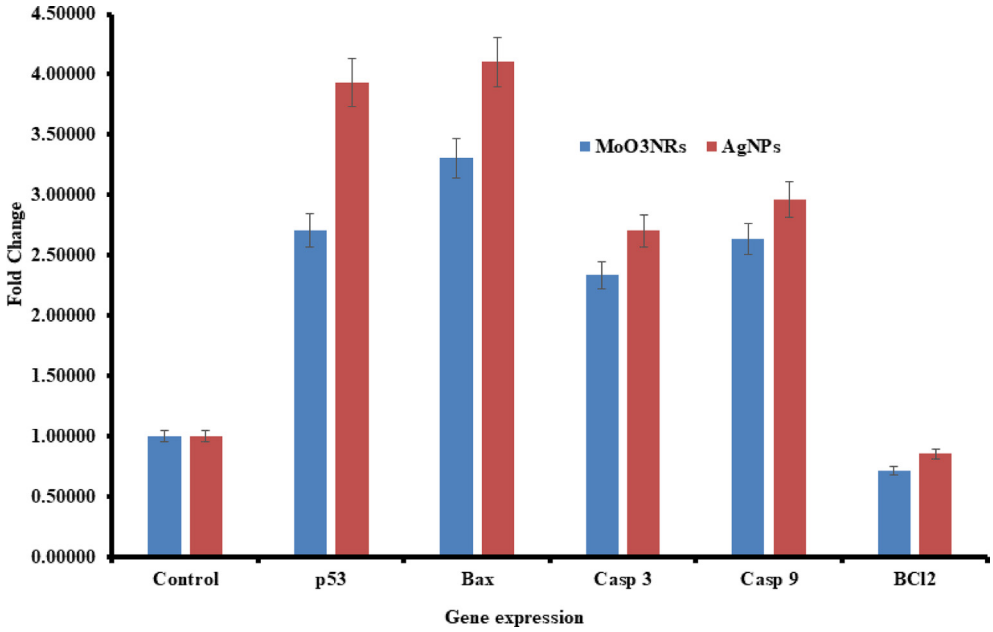


**Fig. 8.** mRNA expression of apoptosis marker genes by RT-PCR analysis in MCF-7 cells with α-$MoO_3$NRs and AgNPs at 50 μg/mL concentration for 24 h. RT-PCR data was achieved with Roche Light Cycler®480 soft-ware (version 1.5). The glyceraldehyde 3-phosphate dehydrogenase (GAPDH) gene was used as a control to normalize data. The data is accessible as the mean ± SD of three identical experiments with three replicates manner. *Significantly different associated with the control group ($p < 0.05$ for each).

expression fold changes are p53 (3.9), bax (4.1), Casp-3 (2.7), Casp-9 (2.9) and Bcl-2 (0.85) respectively. A detailed investigation is required to testify the nanostructures as well as the results represent that NPs induced the apoptotic enzymes (casp-3, Casp-9) in a dose-dependent manner (Fig. 8) (Ahmad et al., 2022).

## 4. Conclusions

The summary of the present work displayed that the α-$MoO_3$ nanorods (diameter ~50–60 nm, length 1–2 μm) and AgNPs (size ~15 nm) were synthesized via solution process and were characterized. The α-$MoO_3$ nanorods and AgNPs were used at low to high concentrations range (1 to 100 μg/mL) against MCF-7 cancer cells, which indicates that the cytotoxicity of MCF-7 cells influence against cancer cells and are dose reliant validated via MTT and NRU assays. The cells in apoptosis were happened with NPs at optimized doses of conc (50 μg/mL). The present work infers that as compared to the α-$MoO_3$ rods, AgNPs have more possibilities and high reactivity against breast cancer cells. These metal based NPs are much effective as compared to available organic compounds and their sustainability required under biological conditions. The study typify that NPs induces the cytotoxicity, apoptosis in MCF-7 cancer cells via p53, Bax, and caspase pathways, whereas Bcl-2 act as an anti-apoptotic marker gene for cancer cells and are consistent with other data's. The ROS generation increased in cancer cells, due to the interaction of α-$MoO_3$ rods and AgNPs. From the entire experiment and their results it suggest that NPs are much effective and are responsible to regulate the growth of cancer cells. The use of nanostructured materials for to control the cancer cells, provides better and substantial approaches as compared to the available existing technologies, with no harmful or side effects due to their biocompatible nature. In future, the different shaped nanostructures have possibility to react directly and quickly to the cancer cells, due to their unique size and small dimension facilitates nanostructures and it can be easily entered in to the cells organelles and reacted fast against cancer cells. The utility of these NPs against cancer studies may possible to reduce the cost of the preparation, also studies reduces the anxiety of surgery for the deprived patient.

## Declaration of Competing Interest

The authors declare that they have no known competing financial interests or personal relationships that could have appeared to influence the work reported in this paper.

## Acknowledgement

The authors extend their appreciation to the Deputyship for Research & Innovation, Ministry of Education in Saudi Arabia for funding this research (IFKSURC-1-3207).

## Appendix A. Supplementary material

Supplementary data to this article can be found online at https://doi.org/10.1016/j.jksus.2023.102843.

## References

Ahmad, J., Wahab, R., Siddiqui, M.A., Saquib, Q., Ahmad, N., Al-Khedhairy, A.A., 2022. Strontium-doped nickel oxide nanoparticles: synthesis, characterization, and cytotoxicity study in human lung cancer A549 Cells. Biol. Trace Elem. Res. 200, 1598–1607.
Al-Khedhairy, A.A., Wahab, R., 2022. Silver nanoparticles: An instantaneous solution for anticancer activity against human liver (HepG2) and breast (MCF-7) cancer cells. Metals 12, 148.
Boing, L., Vieira, M.D.C.S., Moratelli, J., Bergmann, A., Guimarães, A.C.D.A., 2020. Effects of exercise on physical outcomes of breast cancer survivors receiving hormone therapy–A systematic review and meta-analysis. Maturitas 141, 71–81.
Borenfreund, E., Puerner, J.A., 1985. Toxicity determined in vitro by morphological alterations and neutral red absorption. Toxicol. Lett. 24 (2–3), 119–124.
Božinović, K., Nestić, D., Centa, U.G., Ambriović-Ristov, A., Dekanić, A., Bisschop, L.D., Remškar, M., Majhen, D., 2020. In-vitro toxicity of molybdenum trioxide nanoparticles on human keratinocytes. Toxicology 444, 152564.
Breast Cancer Facts & Figures 2019–2020.

Cammarata, F.P., Forte, G.I., Broggi, G., Bravatà, V., Minafra, L., Pisciotta, P., Calvaruso, M., Tringali, R., Tomasello, B., Torrisi, F., Petringa, G., Cirrone, G.A.P., Cuttone, G., Acquaviva, R., Caltabiano, R., Russo, G., 2020. Molecular investigation on a triple negative breast cancer xenograft model exposed to proton beams. Int. J. Mol. Sci. 1, 266337.

Chen, K., Wei, J., Ge, C., Xia, W., Shi, Y., Wang, H., Jiang, X., 2020. Application of auto planning in radiotherapy for breast cancer after breast-conserving surger. Sci. Rep. 10, 10927.

He, X., Zhang, Q., Feng, Y., Li, Z., Pan, Q., Zhao, Y., Zhu, W., Zhang, N., Zhou, J., Wang, L., Wang, M., Liu, Z., Zhu, H., Shao, Z., Wang, L., 2020. Resection of liver metastases from breast cancer: a multicentre analysis. Clin. Transl. Oncol. 22, 512–521.

Indrakumar, J., Korrapati, P.S., 2020. Steering efficacy of nano molybdenum towards cancer: mechanism of action. Biol. Trace Elem. Res. 194, 121–134.

Iqbal, S., Alam, M.F., Atif, M., Amin, N., Ali, A., Shafiq, M., Ismail, M., Hanif, A., Farooq, W.A., 2020. Photodynamic therapy, facile synthesis, and effect of sintering temperature on the structure, morphology, optical properties, and anticancer activity of $Co_3O_4$ nano crystalline materials in the HepG2 cell line. J. Photochem. Photobiol. A: Chem. 386, 112130.

Li, J., Li, M., Tian, L., Qiu, Y., Yu, Q., Wang, X., Guo, R., He, Q., 2020. Facile strategy by hyaluronic acid functional carbon dot-doxorubicin nanoparticles for CD44 targeted drug delivery and enhanced breast cancer therapy. Inter. J. Pharmaceut. 578, 119122.

Mosmann, T., 1983. Rapid colorimetric assay for cellular growth and survival: Application to proliferation and cytotoxicity assays. J. Immunol. Methods 65 (1–2), 55–63.

Nardin, S., Mora, E., Varughese, F.M., Avanzo, F.D., Vachanaram, A.R., Rossi, V., Saggia, C., Rubinelli, S., Gennari, A., 2020. Breast cancer survivorship, quality of life, and late toxicities. Front. Oncol. 10, 864.

Qiu, N., Yang, X., Zhang, Y., Zhang, J., Ji, J., Zhang, Y., Kong, X., Xi, Y., Liu, D., Ye, L., Zhai, G., 2021. A molybdenum oxide-based degradable nanosheet for combined chemo-photothermal therapy to improve tumor immunosuppression and suppress distant tumors and lung metastases. J. Nanobiotechnol. 19, 428.

Siddiqui, M.A., Singh, G., Kashyap, M.P., Khanna, V.K., Yadav, S., Chandra, D., Pant, A. B., 2008. Influence of cytotoxic doses of 4-hydroxynonenal on selected neurotransmitter receptors in PC-12 cells. Toxicol. In Vitro 22 (7), 1681–1688.

Siddiqui, M.A., Kashyap, M.P., Kumar, V., Al-Khedhairy, A.A., Musarrat, J., Pant, A.B., 2010. Protective potential of trans-resveratrol against 4-hydroxynonenal induced damage in PC12 cells. Toxicol. In Vitro 24 (6), 1592–1598.

Wahab, R., Dwivedi, S., Umar, A., Singh, S., Hwang, I.H., Shin, H.S., Musarrat, J., Al-Khedhairy, A.A., Kim, Y.S., 2013. ZnO nanoparticles induce oxidative stress in cloudman S91 melanoma cancer cells. J. Biomed. Nanotech. 9, 441–449.

Wahab, R., Siddiqui, M.A., Saquib, Q., Dwivedi, S., Ahmad, J., Musarrat, J., Al-Khedhairy, A.A., Shin, H.S., 2014. ZnO nanoparticles induced oxidative stress and apoptosis in HepG2and MCF-7 cancer cells and their antibacterial activity. Colloids Surf. B: Bio Interfaces 117, 267–276.

Wahab, R., Khan, F., Ahmad, N., Alam, M., 2020. Molybdenum rods assembled with nanosheets: a high catalytic material for phenol sensing. Mater. Toady Chem. 18, 100347.

Zhao, J., Riediker, M., 2014. Detecting the oxidative reactivity of nanoparticles: a new protocol for reducing artifacts. J. Nanopart. Res. 16 (7), 2493.